

Factorized distorted-wave approximation for the $(e, 2e)$ reaction on atoms: Coplanar symmetric*

I. Fuss, I. E. McCarthy, C. J. Noble, and E. Weigold

Institute for Atomic Studies, The Flinders University of South Australia, Bedford Park, South Australia 5042, Australia

(Received 28 February 1977)

The coplanar symmetric $(e, 2e)$ cross section has been studied in the intermediate-energy region for the valence states of the inert gases He, Ar, and Ne. Experimental measurements at 200, 400, 800, and 1200 eV for He, and at 400, 800, and 1200 eV for Ne and Ar, are compared with calculations based on the factorized half-off-shell distorted-wave impulse approximation. Calculations are carried out using partial-wave-expanded optical-model wave functions which describe elastic scattering for the distorted waves, the eikonal approximation, and the plane-wave approximation. The latter two significantly overestimate the cross sections at small angles and the valence s -orbital cross section relative to the valence p -orbital one. They also predict the small-angle peak in the p -orbital cross section to be at an angle significantly smaller than is observed. Of the two, the eikonal approximation provides the better description of the data. The full calculation, on the other hand, underestimates the cross sections at small angles and the cross section for the more tightly bound s -orbital relative to the small-angle p -orbital cross section. It also underestimates the ratio of the large- to small-angle peak heights in the p -orbital cross section. All three approximations improve as the energy is increased. The full calculation shows that the factorized distorted-wave impulse approximation cannot provide an adequate description of the reaction.

I. INTRODUCTION

In spite of the success of the $(e, 2e)$ reaction¹ in extracting structure information about atoms, molecules, and their ions, the simple eikonal approximations used for distorted waves in the analysis of data have not enabled us to obtain a sufficiently accurate understanding of the validity of the factorized distorted-wave off-shell impulse approximation as a description of the ionization reaction. In the preceding paper² it was shown that the use of partial-wave-expanded distorted waves calculated in an optical-model potential that describes elastic scattering in detail confirms the validity of the approximation in the noncoplanar symmetric kinematic region for light atoms such as neon, although in heavier atoms, it tends to overestimate the effect of absorption for the more tightly bound orbitals.

The coplanar symmetric reaction is a much stricter test of the ionization theory for the following reasons. The unfactorized distorted-wave off-shell impulse approximation¹ gives an amplitude proportional, in the quasi-three-body approximation to

$$M(\vec{k}_A, \vec{k}_B) = n^{1/2} S_f^{(f)/2} \times \langle \chi_A^{(-)}(\vec{k}_A) \chi_B^{(-)}(\vec{k}_B) | t(p^2) | \psi_f(\epsilon_f) \chi_0^{(+)}(\vec{k}_0) \rangle, \quad (1)$$

where the incident and two outgoing momenta are, respectively, \vec{k}_0 , \vec{k}_A , and \vec{k}_B and the energy at which the Coulomb t matrix $t(p^2)$ is evaluated is, in atomic units,

$$\frac{1}{2} p^2 = \frac{1}{8} |\vec{k}_A - \vec{k}_B|^2. \quad (2)$$

This energy varies rapidly with θ —the variable in the present case—but extremely slowly with ϕ —the variable in the noncoplanar symmetric case.

The functions $\chi^{(\pm)}(\vec{k}, \vec{r})$ are distorted waves calculated in optical-model potentials chosen to fit elastic scattering. The knocked-out electron is from the orbital ψ_f which is originally occupied by n electrons. The spectroscopic factor for the observed final state f is $S_f^{(f)}$.

In the plane-wave approximation (1) factorizes exactly into a half-off-shell t matrix element and the Fourier transform $\phi_f(\epsilon_f, \vec{q})$ of the bound-state orbital, where

$$\vec{q} = \vec{k}_0 - \vec{k}_A - \vec{k}_B \quad (3)$$

is the experimentally-measured recoil momentum. The factorized distorted-wave approximation assumes that the distorted waves are sufficiently like plane waves for the factorization to be valid, while the distorted waves are restored in the transform of the bound state. In this approximation

$$M(\vec{k}_A, \vec{k}_B) = n^{1/2} S_f^{(f)/2} \langle \vec{k}' | t(p^2) | \vec{k} \rangle \times \langle \chi_A^{(-)}(\vec{k}_A) \chi_B^{(-)}(\vec{k}_B) | \psi_f(\epsilon_f) \chi_0^{(+)}(\vec{k}_0) \rangle. \quad (4)$$

The factorization is expected to be better for slowly-varying t than for rapidly varying t , although a full calculation including the integrations over the fully off-shell t matrix in the unfactorized approximation is necessary for a complete investigation of this point.

The investigation of the reaction mechanism would not be complete if it were to neglect the fact

that there are Coulomb forces in the three-body final state. The Coulomb forces are allowed for by the effective-charge method of Rudge and Seaton³ and Peterkop.⁴ This is briefly described in Sec. II.

One would expect the simple eikonal approximation¹ to improve as the incident energy is increased. The factorization approximation should therefore improve for the same reason. The energy variation of cross sections is investigated with this question in mind.

The factorized distorted-wave approximation (4) is currently also used for the nuclear analog of the ($e, 2e$) reaction, ($p, 2p$), where it has not been successful⁵ in providing detailed fits to coplanar symmetric angular correlations. The ($e, 2e$) reaction provides a useful analog for ($p, 2p$) since the parameters of the calculation are better known and more-detailed experimental data are available.

This investigation essentially asks the question whether (4) is a good approximation to a breakup reaction where the interactions in the two-body subsystems are quite well known. In order to provide a reasonably complete investigation a number of inert gases, helium, neon, and argon are taken as targets and the energy is varied over the range 200 to 1200 eV for helium, and 400 to 1200 eV for the heavier gases neon and argon.

The problem is formulated in Sec. II. A brief outline of the experimental technique is given in Sec. III and the theoretical and experimental results are presented and discussed in Sec. IV.

II. FORMULATION OF THE PROBLEM

The ($e, 2e$) amplitude was derived in the form (4) in Ref. 1, where each approximation in the reduction of the many-body problem was discussed explicitly. The approximation that could not really be justified, except by the overall success of the theory in fitting data, was that the electron-electron potential is effectively of short range for the symmetric kinematics, which involves close collisions.

It is not necessary to make this approximation if one properly takes into account the Coulomb forces in the three-body final state. In the present work we do this by the method outlined by Rudge.⁶

Effective charges Z_A and Z_B for the electrons detected at A and B are chosen so as to remove the logarithmic singularity in the phase of the ($e, 2e$) amplitude due to the Coulomb forces, which is

$$\lim_{\rho \rightarrow \infty} \exp \left[i \left(\frac{1}{k_A} + \frac{1}{k_B} - \frac{1}{|\vec{k}_A - \vec{k}_B|} - \frac{Z_A}{k_A} - \frac{Z_B}{k_B} \right) \ln 2X\rho \right], \quad (5)$$

where

$$X^2 = k_A^2 + k_B^2. \quad (6)$$

The condition determining the effective charges is therefore

$$\frac{Z_A}{k_A} + \frac{Z_B}{k_B} = \frac{1}{k_A} + \frac{1}{k_B} - \frac{1}{|\vec{k}_A - \vec{k}_B|}. \quad (7)$$

Since the actual charge of the ion is 1, there is a residual Coulomb potential which must be neglected beyond some cutoff radius R_0 . For $r < R_0$ it is included in the distorting potentials for calculating $\chi^{(\pm)}(\vec{k}, \vec{r})$.

The differential cross section is proportional to

$$\sigma = |f(\vec{k}_A, \vec{k}_B)|^2 + |f(\vec{k}_B, \vec{k}_A)|^2 - \text{Re}[f(\vec{k}_A, \vec{k}_B)^* f(\vec{k}_B, \vec{k}_A)], \quad (8)$$

$$f(\vec{k}_A, \vec{k}_B) = -(2\pi)^{-5/2} \exp[i\Delta(\vec{k}_A, \vec{k}_B)] M(\vec{k}_A, \vec{k}_B), \quad (9)$$

$$\Delta(\vec{k}_A, \vec{k}_B) = 2[(Z_A/k_A) \ln(k_A/X) + (Z_B/k_B) \ln(k_B/X)]. \quad (10)$$

The formal inclusion of the Coulomb forces in the three-body final state has been discussed in more detail by McCarthy, Noble, and Sloan.⁷

For the present symmetric kinematics we choose

$$Z_A = Z_B = Z. \quad (11)$$

The effective charge Z is dependent on the angle θ between the outgoing electrons and the incident direction. The computation must therefore be done completely for each angle. We have normally set $Z = 1$, but for some cases we have performed the full computation to show the effect of its inclusion.

The optical-model potentials are calculated according to the prescription of McCarthy, Noble, Phillips, and Turnbull⁸ from Hartree-Fock orbitals.⁹ For the ion, we use the Hartree-Fock orbitals appropriate to an ion with a hole in the orbital from which ionization occurs. There are two parameters in each optical-model potential. These are the static polarizability α and the imaginary potential strength W . For the neutral atom, they are chosen to fit elastic scattering and total reaction cross-section data. For the helium ions, the parameters α and W were derived directly from a combination of experimental and theoretical data. In the absence of such data for the neon and argon ions, the neutral-atom parameters at the appropriate two-body energies were used for the corresponding electron-ion interactions. The bound-state wave function ψ , in Eq. (1) is the Hartree-Fock orbital for the neutral atoms. Computational details are described in the preceding paper.²

Since the averaged eikonal approximation

$$\chi^{(\pm)}(\vec{k}, \vec{r}) = \exp(-\gamma kR) \exp[i(1 + \beta \pm i\gamma)\vec{k} \cdot \vec{r}], \quad (12)$$

$$\beta + i\gamma = (\bar{V} + i\bar{W})/2E, \quad (13)$$

has had considerable success in fitting shapes of coplanar symmetric angular correlations,^{10,11} it is

calculated for comparison purposes with the parameter values $\bar{V} = 10$ eV, $\bar{W} = 5$ eV.

III. EXPERIMENTAL DETAILS

The coplanar electron coincidence spectrometer shown schematically in Fig. 1 has been described in detail in Ref. 1, and only a brief description will be given here. It was mounted on the bottom of a metal bell-jar vacuum chamber and pumped by a 4-in. oil diffusion pump and an associated liquid-nitrogen trap through a port in the bottom plate. Helmholtz coils and μ -metal shielding reduced

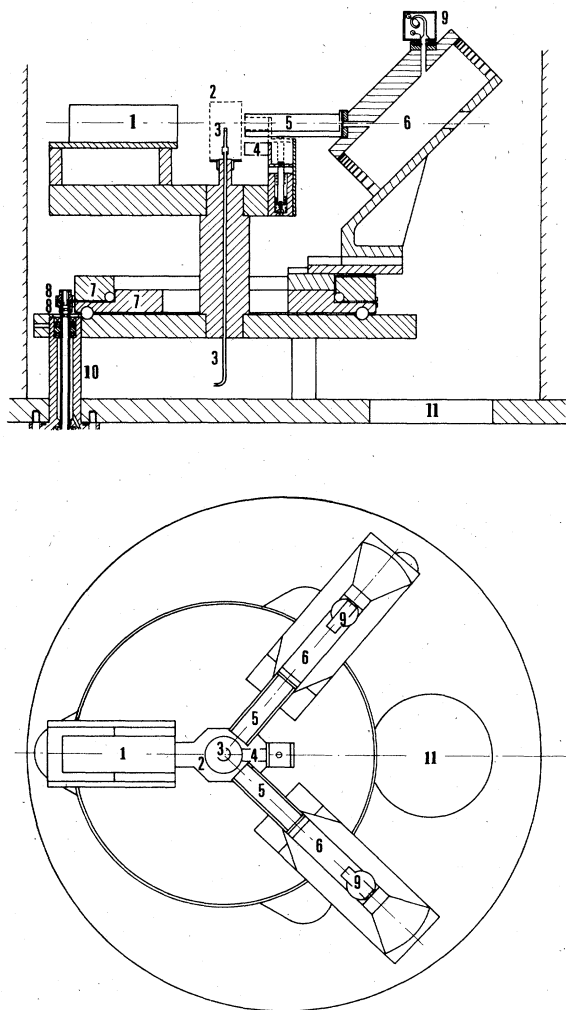


FIG. 1. Coplanar electron coincidence spectrometer showing side and top elevations. 1 is the cylindrical stainless-steel electron gun mount; 2, the grounded interaction region shield; 3, the gas inlet; 4, the retractable Faraday cup; 5, collimators, quadrupole deflectors, and retarding lenses; 6, cylindrical mirror analyzers; 7, concentric turntables; 8, gears; 9, channel electron multipliers; 10, rotating feedthroughs from stepping motor; 11, pumping port.

stray magnetic fields to less than 10 mG within the experimental region.

Two cylindrical mirror analyzers, mounted on concentric turntables and preceded by a collimating and retarding lens system, were used to determine the energies and the polar angles of the emitted electrons. The analyzers were moved in equal and opposite steps by a stepping motor on command from a PDP-11 computer. The full width of the acceptance angle of the collimators was 1.2° .

Target gas of at least 99.9% purity was leaked into the interaction region through a multichannel array placed approximately 1 mm below the horizontal electron beam. Base pressures in the vacuum chamber were approximately 10^{-6} Torr, the experiments being conducted in an ambient pressure in the range $(4-10) \times 10^{-6}$ Torr. The viewing angles of the analyzers must be larger than the effective size of the interaction region, defined by the intersection of the electron and atomic beams. To ensure that this was the case, angular distributions were measured with each analyzer for electrons elastically scattered from argon at several incident energies and compared with well-known measurements.¹² In addition, the angular distributions of secondary electrons produced in electron impact ionization of helium were compared with the data of Oda and co-workers.¹³ The excellent agreement obtained with the elastic and double differential cross sections measured by other techniques showed that the viewing angle of each detector was indeed larger than the interaction region and that no geometric corrections need be applied to the coincidence count rate as a function of the angle.

The electron beam current and atomic beam density had long-term stabilities of a few percent. Changes in atomic or electron beam densities were compensated for by feeding the corresponding ambient pressure or current signals through a voltage-to-frequency converter to a preset scaler, which controlled the experiment. The signal processing and fast-timing electronics was similar to that described previously.¹ The timing resolution was typically 6 nsec, the accidental coincidence window being set at approximately 10 times the coincidence window width in order to reduce errors in correcting for the accidental coincidences in the "coincidence" window.

The experiment was carried out in two modes. In the first, the coincidence count rate was measured at a given angle as a function of the incident energy with fixed outgoing energies. In the second, the angular correlations for the ion eigenstates of interest were measured by having the computer set the corresponding incident energies and angles. At each energy and angle the computer recorded the counts in the coincidence and background scalers

after being triggered by the preset scaler, subtracted the background counts from the coincidence counts (taking account of the relative channel widths), calculated the statistical error, set a new beam energy and new angles for the analyzers, and then restarted the scalers. The time spent collecting data at a given energy and angle could therefore be kept quite brief, ensuring that a complete scan through all the energies and angles was short in comparison to any long-term drifts of the electron current or target gas density. A cumulative result of counts versus energy and angle was thus obtained. A check was maintained on the consistency of the data by having the data printed out at regular intervals after a given number of scans.

IV. RESULTS AND DISCUSSION

A. Helium

The results at 200, 400, 800, and 1200 eV for helium are presented in Figs. 2-5. The experimental data all show a maximum close to the angle θ_0 for which the ion recoil momentum q is zero. For an $l=0$ orbital this is the most probable value of the electron momentum. As the energy increases, the peak angle approaches 45° . The experimental results and plane-wave and eikonal

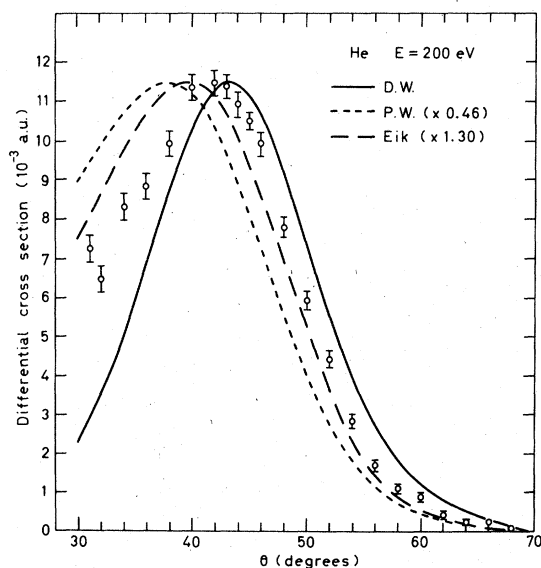


FIG. 2. 200-eV coplanar symmetric ($e, 2e$) cross section (in units of $a_0^2/\text{hartree sr}^2$) for helium compared with the factorized distorted-wave off-shell impulse approximation using plane waves (---), eikonal approximation (— · —), and partial-wave-expanded distorted waves (—). The peaks in the experimental data and the calculations have been normalized to the value given by the full distorted-wave calculation.

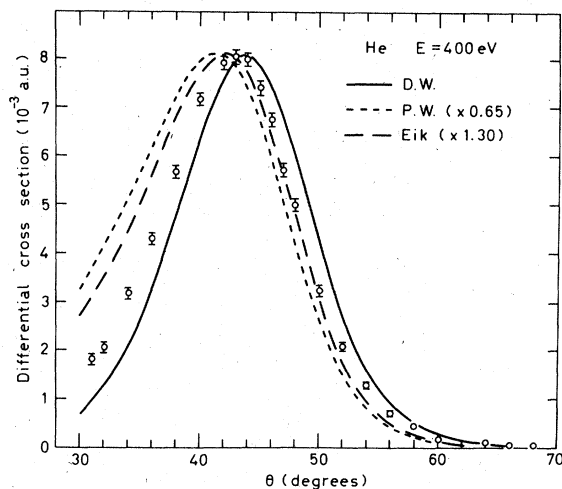


FIG. 3. 400-eV coplanar symmetric ($e, 2e$) cross section (in units of $a_0^2/\text{hartree sr}^2$) for helium compared with the factorized distorted-wave off-shell impulse approximation using plane waves (---), eikonal approximation (— · —), and partial-wave-expanded distorted waves (—). The peaks in the experimental data and the calculations have been normalized to the value given by the full distorted-wave calculation.

calculations have all been normalized to give the same peak height as that predicted by the full distorted-wave calculation.

At all energies, the plane-wave and full partial-

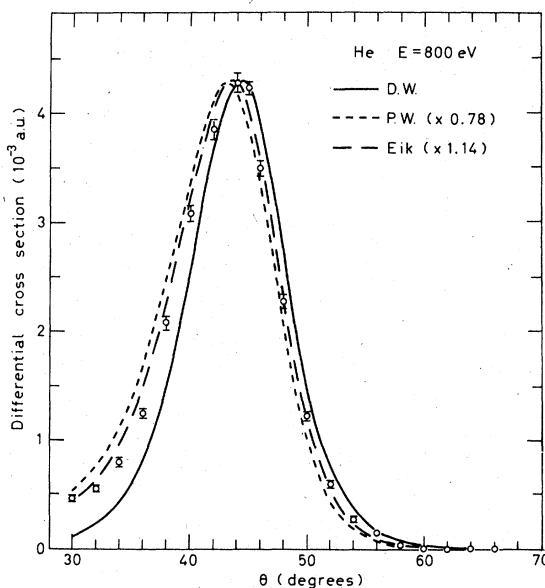


FIG. 4. 800-eV coplanar symmetric ($e, 2e$) cross section (in units of $a_0^2/\text{hartree sr}^2$) for helium compared with the factorized distorted-wave off-shell impulse approximation using plane waves (---), eikonal approximation (— · —), and partial-wave-expanded distorted waves (—). The peaks in the experimental data and the calculations have been normalized to the value given by the full distorted-wave calculation.

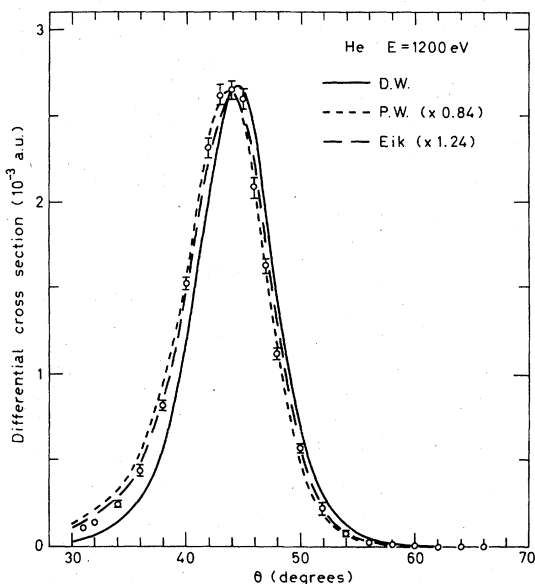


FIG. 5. 1200-eV coplanar symmetric ($e, 2e$) cross section (in units of $a_0^2/\text{hartree sr}^2$) for helium compared with the factorized distorted-wave off-shell impulse approximation using plane waves (---), eikonal approximation (- -), and partial-wave-expanded distorted waves (-). The peaks in the experimental data and the calculations have been normalized to the value given by the full distorted-wave calculation.

wave-expanded distorted-wave calculations lie on opposite sides of the experimental results. The plane-wave approximation consistently predicts the peak angle at a smaller angle than observed, whereas the full calculations predict precisely the

opposite. Similarly, the plane-wave calculations overestimate the cross sections at the smaller angles but underestimate them at larger angles. The full calculation predicts the reverse.

The eikonal approximation, however, gives a very good fit to the experimental results over the whole angular and energy range. It allows for some distortion of the electron waves and predicts cross sections which lie between those given by the two other calculations. It is surprising that the full partial-wave-expanded distorted waves lead to a much inferior fit to the data. The results of all the approximations approach each other and the data as the energy is increased.

B. Neon

The results for neon at 400, 800, and 1200 eV are presented in Figs. 6–8. The data at each energy have been normalized in order to give the same forward peak height for the $2p$ differential cross section as that given by the distorted-wave calculations (full curve). The $2p$ angular correlation displays two maxima, one at $\theta < 45^\circ$ (the forward peak) and one at $\theta > 45^\circ$ (the backward peak), which reflect the momentum distribution of the ejected electron. The angle θ_0 at which $q = 0$ is in all cases slightly smaller than 45° due to the finite separation energy of an electron ejected from the $2p$ orbital. The separation energy spectrum for neon in the valence region can be seen in the preceding paper.² At angles $\theta < \theta_0$, the ejected electron has momenta in the direction of the incoming electron, and the center-of-mass energy is therefore smaller than that for backward collisions, i.e., $\theta > \theta_0$.

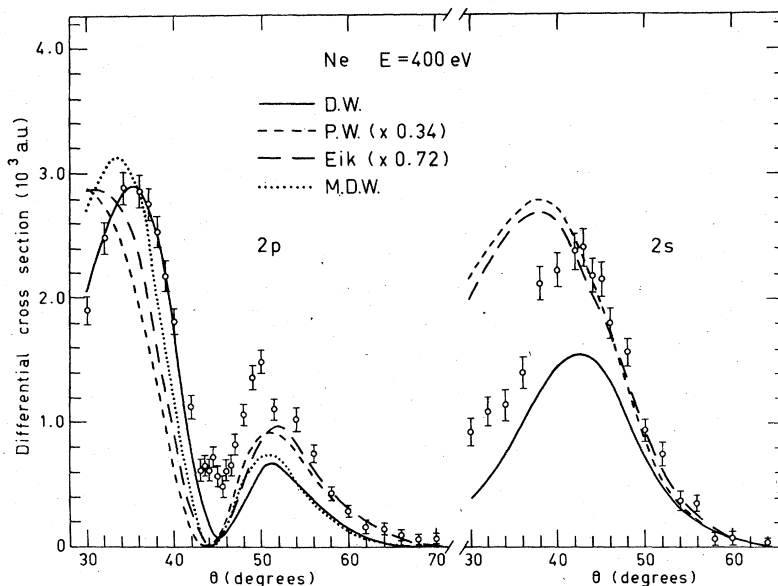


FIG. 6. 400-eV coplanar symmetric ($e, 2e$) cross section (in units of $a_0^2/\text{hartree sr}^2$) for the valence orbitals of neon compared with the factorized distorted-wave off-shell impulse approximation using plane waves (---), the eikonal approximation (- -), and full partial-wave-expanded distorted waves. The experimental data have been normalized to the $2p^{-1}$ forward maximum of the full distorted-wave calculation for the $2p^{-1}$ transition. A modified full distorted-wave (MDW) calculation with the final-state effective charge of zero rather than one, but with the Coulomb phases left in, is shown by the dotted curve.

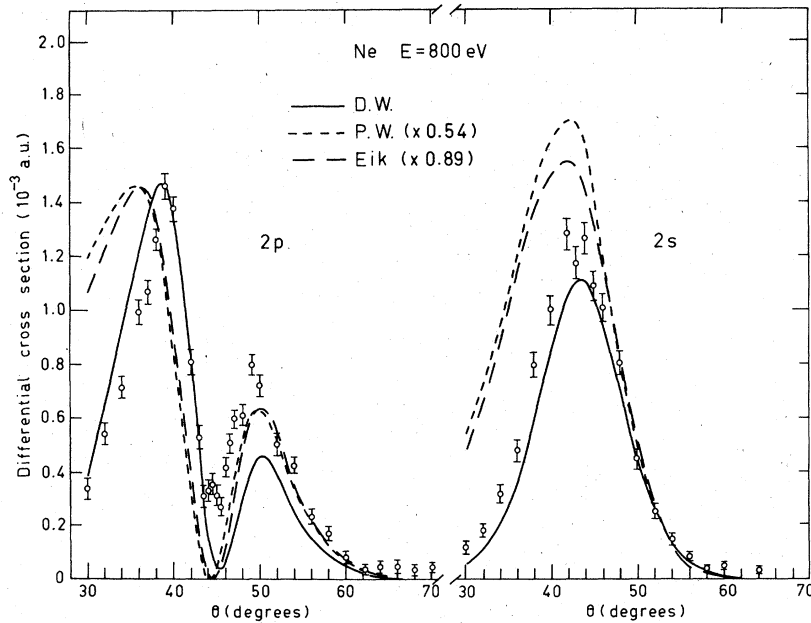


FIG. 7. 800-eV coplanar symmetric $(e,2e)$ reaction for the valence orbitals of neon compared with the factorized distorted-wave off-shell impulse approximation. Symbols and normalization are the same as in Fig. 6.

This decrease in the electron-electron center-of-mass energy with angle θ [Eq. (2)] accounts for the cross section at $\theta < \theta_0$ being considerably larger than the cross section at the corresponding angle $\theta > \theta_0$ with the same value of q . In the expression for the cross section [Eq. (4)] this is accounted for by the energy dependence of the Coulomb t matrix.

The positions of the two peaks in the angular correlation for the ejection of an electron from the p orbital are very well described by the full distorted-wave calculation. The calculation, however,

does not obtain the correct ratio of peak heights, seriously underestimating the relative height of the backward peak. At 400 eV, a modified distorted-wave (MDW) calculation was carried out also with the effective charge Z in the exit channel put equal to zero rather than unity. The results obtained differ only slightly from the full distorted-wave calculation. The *ad hoc* inclusion of the Coulomb phase [see Eq. (6), preceding paper] in the modified calculation leads to a significant change in the cross section. This is shown as the dotted curve

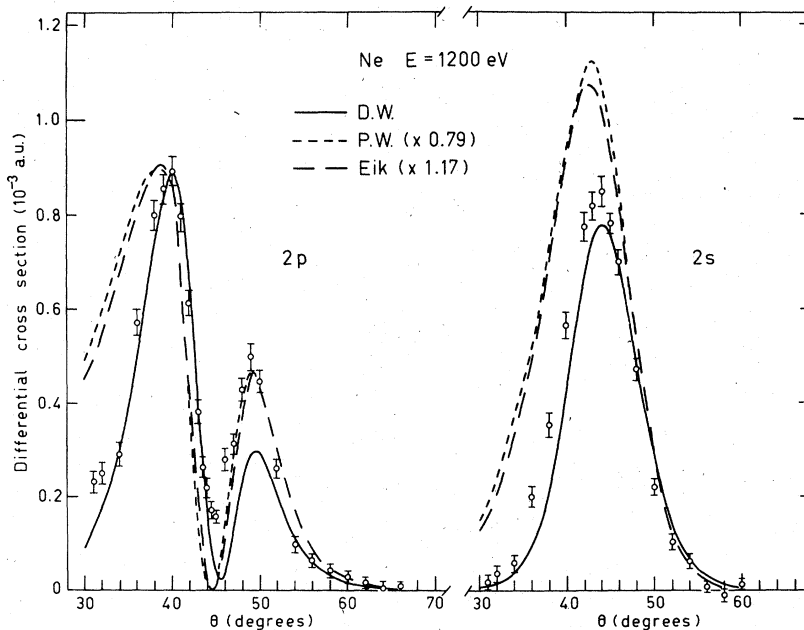


FIG. 8. 1200-eV coplanar symmetric $(e,2e)$ reaction for the valence orbitals of neon compared with the factorized distorted-wave off-shell impulse approximation. Symbols and normalization are the same as in Fig. 6.

in Fig. 6. In this calculation the forward peak is shifted to smaller angles and the relative height of the backward peak is significantly increased. Although the improvement in the fit to the data is spurious it strongly suggests that the deficiencies in the present calculation are due to the use of the factorization approximation.

The plane-wave and eikonal approximations (short and long dashes) are in serious disagreement with the data over the position of the forward peak at all energies. They predict peaks at angles much smaller than those observed in the experiment. It is rather surprising, however, that they both give a much better forward-to-backward peak height ratio than is given by the full calculation. In fact, the peak height ratios predicted by the plane-wave and eikonal approximations are in excellent agreement with the data at all energies. The improvement over the shape of the plane-wave cross sections introduced by the eikonal approximation is relatively minor. The eikonal approximation, however, does obtain an absolute cross section in much better agreement with the full calculation.

All three calculations predict a $2p^{-1}$ cross-section minimum at or near $\theta = \theta_0$ much smaller than that observed experimentally. Inclusion of the finite angular resolution, approximately 0.6° full width at half maximum (FWHM), has an almost negligible effect on the cross-section shape, and part of the discrepancy between theory and experiment at $\theta \approx \theta_0$ is real at all energies.

The valence p -orbital of the inert gases is not significantly split among ion eigenstates and in neon the valence s -orbital is also not significantly split.¹ The $2s$ data shown in Figs. 6–8 are the

cross sections for the ion eigenstate with separation energy of 48.5 eV. The excitation cross section for this state, which contains approximately 96% of the strength of the $2s$ orbital, is measured relative to the ground state ($2p^{-1}$) transition.

With the present normalization of the data to the forward $2p$ peak, the distorted-wave calculation underestimates the $2s$ cross section at all energies, particularly at the smaller angles. It nevertheless describes the shapes quite well and gives the correct position for the peaks in the cross sections. (In contrast to the case for the p orbital, for an s orbital the most probable value of the momentum q is zero.) Figures 6–8 also show that the approximation improves as the energy is increased.

The eikonal and plane-wave approximations seriously overestimate the magnitude of the $2s$ cross section at all energies, although they also improve as the energy is increased. Both give the wrong cross-section shape, becoming worse as the angle θ decreases. The eikonal approximation is again marginally better than the plane-wave approximation. If the plane-wave and eikonal approximation are applied only to angles $\theta \geq 45^\circ$, as was done in Ref. 10, the agreement with the data is quite good.

C. Argon

The differential cross sections obtained for the argon valence $3p$ and $3s$ transitions at 400, 800, and 1200 eV are presented in Figs. 9–11, respectively. As in neon, the argon valence $3p$ strength is not significantly split among ion eigenstates, and the experimental data are for the ground-state

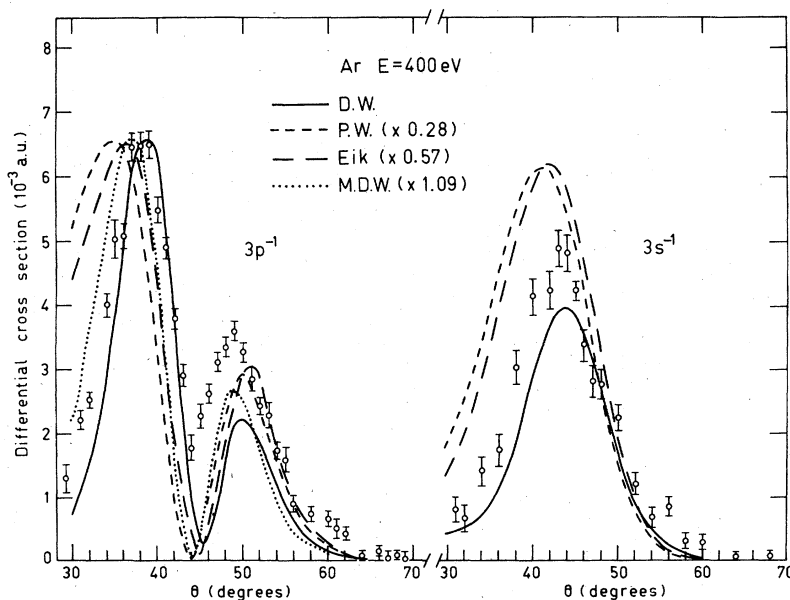


FIG. 9. 400-eV coplanar symmetric ($e, 2e$) reaction for the valence orbitals of argon compared with the factorized distorted-wave off-shell impulse approximation. Symbols and normalization are the same as in Fig. 6.

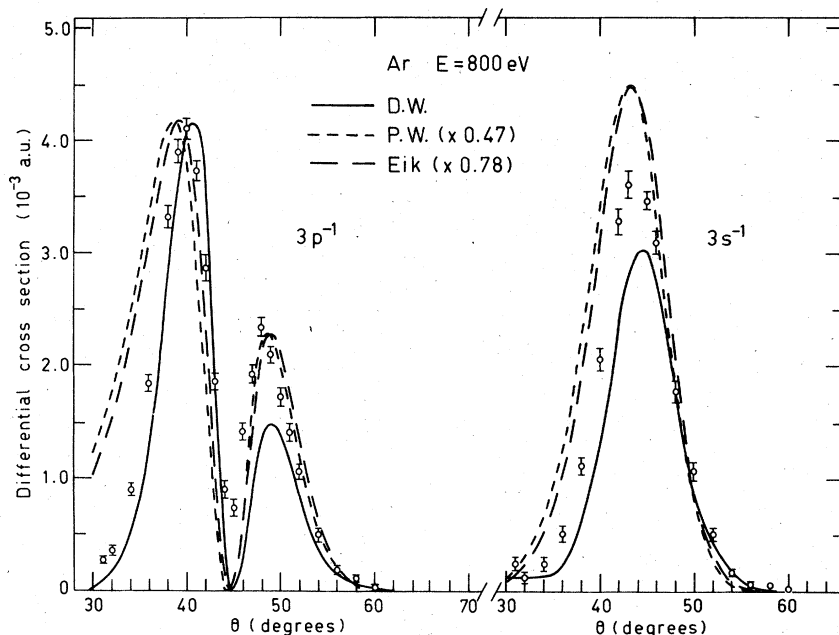


FIG. 10. 800-eV coplanar symmetric $(e, 2e)$ reaction for the valence orbitals of argon compared with the factorized distorted-wave off-shell impulse approximation. Symbols and normalization are the same as in Fig. 6.

transition. The $3s$ orbital is, however, significantly split,¹ and the experimental data shown in Figs. 9–11 represent the total $3s^{-1}$ strength, the cross section having been summed over all the ion eigenstates containing the $3s^{-1}$ orbital. The experimental cross sections have again been normalized to the maximum in the forward peak of the full distorted-wave result for the $3p^{-1}$ transition. Only the statistical errors (one standard deviation) are shown in the figures. The absolute magnitude of

the $3s^{-1}$ cross section (relative to the normalized $3p^{-1}$ cross section) has an additional systematic normalization error of 3% at 400 eV, 4% at 800 eV, and 5% at 1200 eV.

For the $3p^{-1}$ transition, the plane-wave and eikonal approximations again give a very poor fit to the data at forward angles ($\theta < \theta_0$). They predict cross sections which are significantly too large at the most forward angles and put the forward peak at too small an angle. The backward peaks are at

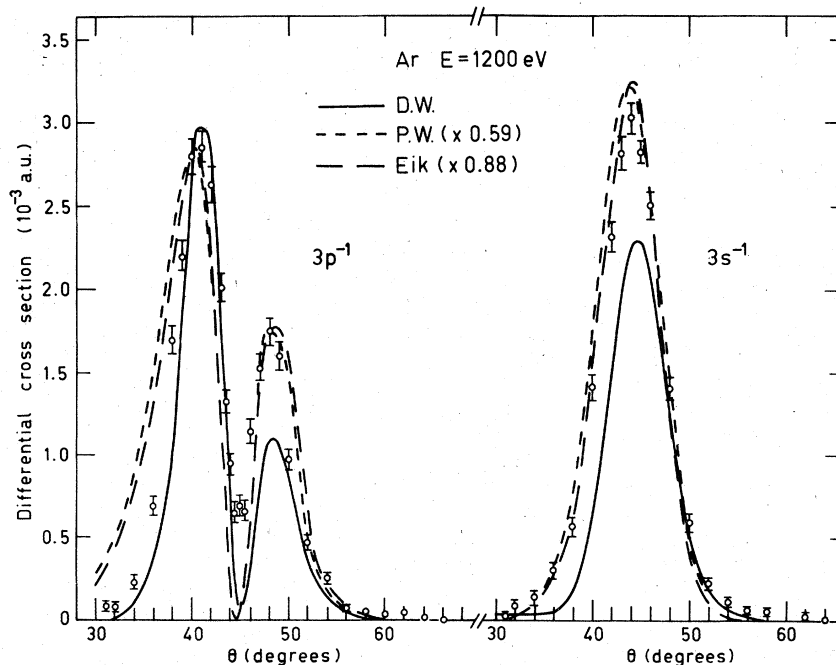


FIG. 11. 1200-eV coplanar symmetric $(e, 2e)$ reaction for the valence orbitals of argon compared with the factorized distorted-wave off-shell impulse approximation. Symbols and normalization are the same as in Fig. 6.

slightly too large an angle, although the peak height ratios are quite well given by both approximations. As for neon, the eikonal approximation gives a marginally better shape and significantly different magnitude for the cross section compared to the plane-wave result.

The distorted-wave calculation (full line) generally lies on the other side of the experimental points. It predicts a cross section which is too low at the most forward angles and significantly underestimates the relative magnitude of the backward peak. It is more successful than the plane-wave and eikonal approximations in giving the positions of the peaks, although the introduction of the full distorted waves seem to "overcorrect" rather more than was the case for neon. As the energy increases from 400 to 1200 eV, all the approximations improve considerably.

At 400 eV (Fig. 9), we have again included the results of an *ad hoc* modified distorted-wave calculation as was done for neon. Surprisingly the fit is again marginally improved.

Figures 9–11 show similar trends for the argon $3s^{-1}$ cross section to those observed in the case of the neon valence- s transition. The plane-wave and eikonal approximations both significantly overestimate the cross section, particularly at the lower energies and forward angles. With the present normalization of the data to the forward $3p^{-1}$ peak, the full distorted-wave calculation again "overcorrects" and obtains a cross-section value below that observed experimentally, particularly over the forward angular region. As was the case for helium and neon, the plane-wave and eikonal approximations improve as the energy is increased.

V. SUMMARY

We have shown that the measurement of symmetric coplanar ($e, 2e$) cross sections in the intermediate-energy region provides a sensitive test of the theoretical models developed for describing the reaction. The experimental data are compared with the results of calculations using the factorized distorted-wave off-shell impulse approximation. Three approximations are used: the full partial-wave-expanded distorted-wave calculation, and the plane-wave and eikonal approximations. For the latter two approximations, factorization is valid.

For helium, the plane-wave and full distorted-wave calculations fall on opposite sides of the data at all energies. The plane-wave approximation predicts cross sections which are too large at the smaller angles and too small at the larger angles ($\theta \geq \theta_0$). The full calculation, on the other hand, shifts the peak in the angular correlation too far back and depresses the forward-angle cross sec-

tion too much. The simple eikonal approximation, which allows for some distortion of the electron waves, actually gives a very good description of all of the data.

At all energies for both neon and argon, the plane-wave and eikonal approximations consistently predict cross sections which are too large at the most forward angles and shift the forward ($\theta < \theta_0$) peak of the valence- p transition to angles smaller than those observed in the data. These approximations also obtain a significantly too-large magnitude for the valence- s cross section, again particularly at forward angles. The eikonal approximation gives a somewhat better fit to the data, although neither is adequate even at the highest energy (1200 eV) employed in the present investigation. The full distorted-wave calculation again overcorrects in one sense. It obtains cross sections which are somewhat too small at forward angles, and it underestimates the strength of the valence- s transition. This latter failure was also observed in the noncoplanar symmetric data reported in the preceding paper.² It also seriously overestimates the forward-to-backward peak height ratios in the valence- p cross sections.

It is interesting to compare the coplanar results for neon with the noncoplanar results reported in the preceding paper. In the noncoplanar case, the full distorted-wave calculation gives a very good description of the data, giving both the shapes and relative magnitudes of the $2p$ and $2s$ cross sections. The noncoplanar geometry is therefore obviously better suited for obtaining structure information on the target system.

In brief, the factorized distorted-wave cross section does not adequately describe the coplanar data even when calculated using the full partial-wave formalism. Moreover, a study of the effect on the calculated ($e, 2e$) angular correlations resulting from variations in the optical-model wave functions indicates that theory and experiment are unlikely to be reconciled by any reasonable choice of optical-model parameters. The results are generally insensitive to such changes. However, the modified distorted-wave calculations described in this paper and studies of the ($p, 2p$) reaction using similar methods¹⁴ suggest that the remaining discrepancies may be largely due to the use of the factorization approximation. Hence, despite the successes of the present method, it seems that in order to completely assess the validity of the distorted-wave off-shell impulse approximation, it will be necessary to evaluate the unfactored amplitude given by Eq. (1). This is especially the case in the coplanar geometry where the Coulomb t matrix varies rapidly with angle. Such a calculation would of course be quite formidable. We are,

nevertheless, presently investigating possible methods for performing this computation. Initial work indicates that some significant advantages may be obtained by the use of momentum-space techniques.

ACKNOWLEDGMENTS

The authors would like to thank Dr. A. J. Dixon and Dr. S. T. Hood for their assistance during various phases of this work.

*Work supported by the Australian Research Grants Committee.

¹I. E. McCarthy and E. Weigold, *Phys. Rep.* **27C**, 276 (1976).

²A. J. Dixon, I. E. McCarthy, C. J. Noble, and E. Weigold, preceding paper, *Phys. Rev. A* **17**, 597 (1978).

³M. R. H. Rudge and M. J. Seaton, *Proc. R. Soc. A* **283**, 262 (1965).

⁴R. K. Peterkop, *Opt. Spectrosc.* **13**, 87 (1962).

⁵R. K. Bhowmik, Ph.D. thesis (University of Maryland, 1974).

⁶M. R. H. Rudge, *Rev. Mod. Phys.* **40**, 564 (1968).

⁷I. E. McCarthy, C. J. Noble, and I. H. Sloan (unpublished).

⁸I. E. McCarthy, C. J. Noble, B. A. Phillips, and A. D. Turnbull, *Phys. Rev. A* **15**, 2173 (1977).

⁹E. Clementi and C. Roetti, *At. Data Nucl. Data Tables* **14**, 177 (1974); P. Bagus, *Phys. Rev.* **139**, A619 (1965).

¹⁰A. Ugbabe, E. Weigold, and I. E. McCarthy, *Phys. Rev. A* **11**, 576 (1975).

¹¹R. Camilloni, G. Stefani, A. Giardini-Guidoni, R. Tiribelli, and D. Vinciguerra, *Chem. Phys. Lett.* **41**, 17 (1976).

¹²B. R. Lewis, J. B. Furness, P. J. O. Teubner, and E. Weigold, *J. Phys. B* **7**, 1083 (1974).

¹³N. Oda, *Radiat. Res.* **64**, 80 (1975).

¹⁴W. Thwin (private communication).